

# Heat transfer property of thin-film encapsulation for OLEDs

Jongwoon Park\*, Hyokyun Ham, Cheolyoung Park

*OLED Lighting Team, National Center for Nanoprocess and Equipment, Korea Institute of Industrial Technology, Gwangju 500-480, Republic of Korea*

## ARTICLE INFO

### Article history:

Received 13 July 2010

Received in revised form 16 November 2010

Accepted 26 November 2010

Available online 7 December 2010

### Keywords:

Organic light-emitting diodes

Thin-film encapsulation

Heat transfer

## ABSTRACT

We investigate the heat transfer property of thin-film encapsulation (TFE) for organic light-emitting diodes (OLEDs). It is demonstrated that the TFE combined with a flexible heat sink shows better thermal performance, compared with the epoxy-filled glass encapsulation and the conventional glass encapsulation. By way of experiments and simulations, we verify that the multi-heterojunction configuration and the low thermal conductivity of the polymer layer in the TFE film have no impact on the thermal performance. Furthermore, we find through simulations that a significant temperature gradient appears inside the TFE layers only when the thermal conductivity of the polymer is lower than  $1 \times 10^{-3}$  W/m K. This enables us to perform design optimization of the TFE configuration with relaxed heat dissipation.

© 2010 Elsevier B.V. All rights reserved.

## 1. Introduction

Organic light-emitting diodes (OLEDs) have attracted much attention for their potential applications in flat panel lightings and backlight units of flat panel displays [1,2]. One of the key issues of OLEDs is to protect them from oxygen and moisture. To this end, various encapsulation techniques have been studied. The most commonly used method utilizes UV-cured epoxy along with a desiccant inside the glass-capped OLED device (hereinafter referred to as a glass encapsulation) [3]. Recently, many studies have been made on a thin-film encapsulation (TFE) [4–9]. It is required to have a water vapor transmission rate (WVTR) of below  $10^{-6}$  g m<sup>-2</sup> day<sup>-1</sup> to achieve the lifetime of OLEDs above 10,000 h. Of many TFE methods, TFE based on vacuum based organic/inorganic multi-layers is very promising as a gas diffusion barrier [4,10,11].

Meanwhile, heat dissipation is another key issue for flat panel OLED lighting applications. In analogy to the conventional lighting sources such as bulbs, fluorescent lamps, and inorganic LEDs, flat panel OLED lightings generate a great deal of heat. Unlike inorganic LEDs that have a long heat transfer pathway due to the packaging issue, how-

ever, OLEDs have a very short one between the internal heat source (i.e., light-emitting active area) and the outer device surface; namely, the heat difference between them is very small. This facilitates heat dissipation of OLEDs without using a bulk heat sink. Even so, the Joule heating problem is always parasitic on the devices. Due to Joule heating induced by high current injection during operation, there arise a reduction of luminance, short lifetime, and large spectral shift of OLEDs. To suppress the thermal degradation of organic molecules, the use of a heat sink is inevitable. Such a heat sink is desirable to be slim in such a way as to show up the salient feature of ultra-thin OLEDs.

For bottom-emitting OLED lighting panels, heat transfers through the encapsulation layers to the heat sink. As such, encapsulation need allow high gas diffusion barrier while simultaneously meeting heat transfer requirements. The epoxy seal of the glass encapsulation may not be good moisture barrier. Besides, the glass encapsulation may show poor thermal performance as nitrogen gas resides inside the device, separating a heat sink from the OLED device without any contact involved between them. One may come up with an advanced glass encapsulation where a glass cover is filled with a thermally conductive epoxy through which a heat sink is in contact with the OLED device (hereinafter referred to as an epoxy-filled glass encapsulation). In this case, a significant temperature

\* Corresponding author. Tel.: +82 62 600 6520; fax: +82 62 600 6509.  
E-mail address: [pjwup75@kitech.re.kr](mailto:pjwup75@kitech.re.kr) (J. Park).

Glass	ITO (150nm)	$\alpha$ -NPD (70nm)	Alq <sub>3</sub> (45nm)	Aluminum (150nm)	Al <sub>2</sub> O <sub>3</sub> (50nm)	Polymer (500nm)	Al <sub>2</sub> O <sub>3</sub> (50nm)	Polymer (500nm)	Al <sub>2</sub> O <sub>3</sub> (50nm)	Polymer (500nm)	Al <sub>2</sub> O <sub>3</sub> (50nm)	Copper-heat sink
-------	-------------	----------------------	-------------------------	------------------	---------------------------------------	-----------------	---------------------------------------	-----------------	---------------------------------------	-----------------	---------------------------------------	------------------

**Fig. 1.** Schematic view of the layer structure of a thin-film encapsulated OLED.

gradient may appear if the thermal conductivity of epoxy is low [12]. In this respect, the TFE structure shown in Fig. 1 would be in good combination with a heat sink provided that its barrier property is satisfactory since the TFE layer is extremely thin (several  $\mu\text{m}$ ). However, it still concerns us in respect that the TFE layer is composed of alternating organic/inorganic materials (namely, a multi-heterojunction is entailed) and furthermore organic (polymer) materials have relatively low thermal conductivity, which may degrade the heat transfer property. Though many researches on the encapsulation technologies are available in the open literature, yet not much has been reported on their thermal property.

This paper is written with the following objectives. We make a comparative analysis of those encapsulation methods in terms of the heat transfer property. In the presence of a flexible heat sink, it is addressed that the TFE shows the best thermal performance, followed by the epoxy-filled glass encapsulation and then the conventional glass encapsulation. We have also implemented a 1D numerical model and performed numerical simulations of OLEDs to study more systematically the thermal property of the TFE configuration. It is found that the multi-heterojunction of the TFE structure and the low thermal conductivity of a polymer material therein have no impact on the thermal performance.

## 2. Model

In this study, the OLED structure (Fig. 1) consists of a 150-nm-thick indium-tin-oxide (ITO) pre-coated on a glass substrate, 70-nm-thick N,N'-diphenyl-N,N'-bis(1-naphthyl)-1-1'-biphenyl-4,4''diamine ( $\alpha$ -NPD) for a hole transport layer (HTL), 45-nm-thick tris-(8-hydroxyquinoline) aluminum (Alq<sub>3</sub>) for an electron transport layer (ETL), 1-nm-thick lithium fluoride (LiF) for an electron injection layer (EIL), and 150-nm-thick aluminum (Al) for cathode. The TFE layer is composed of alternating inorganic (50-nm-thick Al<sub>2</sub>O<sub>3</sub>)/organic (500-nm-thick polymer) multilayers. With attempt to capture the heat generation and transfer inside the OLED device, we have implemented a comprehensive 1D numerical model [13–16] in which Poisson's equation, drift–diffusion equation, and heat flow equation are coupled to one another.

### 2.1. Poisson's equation

$$\frac{\partial E(x, t)}{\partial x} = \frac{q}{\epsilon_0 \epsilon_r} (p(x, t) - n(x, t) + N_D - N_A) \quad (1)$$

where the variable  $E$  denotes the electric field,  $n$  and  $p$  the electron and hole densities, respectively, and  $N_D$  and  $N_A$  the donor and acceptor impurity concentrations, respectively.

### 2.2. Drift–diffusion equation

$$\begin{aligned} \frac{\partial n(x, t)}{\partial t} &= \frac{1}{q} \frac{\partial J_n(x, t)}{\partial x} - r(x, t)n(x, t)p(x, t) \\ \frac{\partial p(x, t)}{\partial t} &= -\frac{1}{q} \frac{\partial J_p(x, t)}{\partial x} - r(x, t)n(x, t)p(x, t) \end{aligned} \quad (2)$$

where

$$\begin{aligned} J_n(x, t) &= q\mu_n(x, t)n(x, t)E(x, t) \\ J_p(x, t) &= q\mu_p(x, t)p(x, t)E(x, t) \end{aligned} \quad (3)$$

with the variable  $\mu_n$  defined as the electron mobility, and  $\mu_p$  the hole mobility. The degree of disorder of the organic molecules is reflected in the field- and temperature-dependent carrier mobility expressed as [17,18]

$$\mu(E(x, t), T) = \mu_0(T) \exp \left( \sqrt{\frac{E(x, t)}{E_0(T)}} \right) \quad (4a)$$

where

$$\mu_0(T) = \mu_A \exp \left( -\frac{\Delta}{kT} \right) \quad (4b)$$

$$E_0^{-1/2}(T) = D_m \left( \frac{1}{kT} - \frac{1}{kT_0} \right) \quad (4c)$$

with  $\mu_0(T)$  defined as the zero-field temperature-dependent mobility,  $\mu_A$  a constant,  $\Delta$  the activation energy,  $E_0(T)$  the temperature-dependent characteristic field, and  $D_m$  and  $T_0$  material-related constants. The recombination rate  $r$  is expressed in the Langevin form [19]

$$r(x, t) = q(\mu_n(x, t) + \mu_p(x, t))/\epsilon_0 \epsilon_r. \quad (5)$$

### 2.3. Heat flow equation

$$\begin{aligned} C \frac{\partial T(x, t)}{\partial t} &= \frac{\partial}{\partial x} \left( k(x, t) \frac{\partial T(x, t)}{\partial x} \right) \\ &+ \left[ \frac{J_n(x, t)^2}{q\mu_n(x, t)n(x, t)} + \frac{J_p(x, t)^2}{q\mu_p(x, t)p(x, t)} \right] \end{aligned} \quad (6)$$

where  $C$  is the volumetric heat capacitance and  $k$  is the thermal conductivity. The second term in the right-hand side of Eq. (6) represents the Joule heating. The thermal conductivity is assumed to be independent of temperature. Dirichlet boundary condition has been applied at the air/heat sink interface. In the simulation, the ambient temperature was assumed to be 300 K. For simplicity, the thermoelectric effects such as the Seebeck effect and the Peltier effect are not considered in the model. The model is capable of capturing the temperature-dependent OLED behaviors by solving the equation governing the electrical behaviors and the heat flow equation, which are coupled to each other through the temperature-dependent carrier mobility (Eq. (4)). The solutions to the governing equations are obtained in a self-consistent manner. Table 1 lists the

**Table 1**  
Material parameter values.

Layer	$\mu_{0,n}$ (cm <sup>2</sup> /V s)	$\mu_{0,p}$ (cm <sup>2</sup> /V s)	$E_{0,n}$ (V/cm)	$E_{0,p}$ (V/cm)
HTL ( $\alpha$ -NPD)	$1 \times 10^{-8}$	$4.3 \times 10^{-4}$	$1 \times 10^5$	$1 \times 10^6$
ETL (Alq <sub>3</sub> )	$1.2 \times 10^{-6}$	$0.12 \times 10^{-6}$	$1959 \times 10^3$	$1959 \times 10^3$

parameter values related to carrier mobilities [14], which are typical for such a device with the material system chosen.


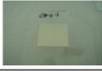




### 3. Results and discussion

For experiments, we have employed a Polynetwork flexible heat sink (PN-FHB050N) [20] in the form of bonding sheet. It consists of a 50- $\mu$ m-thick copper sheet and 35- $\mu$ m-thick thermal radiation layer. The bonding sheet has the thermal conductivity of 0.86 W/m K. After depositing organic and cathode layers, we have formed alternating Al<sub>2</sub>O<sub>3</sub>/monomer layers using Barix™ thin-film encapsulation equipment. Alumina layers are deposited by reactive sputtering of an alumina target. Polymer layers are deposited by organic acrylate evaporation and condensation, followed by a UV cure. The alumina layers form the basis of the moisture and oxygen barrier. Alternating polymer layers provide a smooth surface to facilitate defect free alumina deposition. Shown in Fig. 2 is the scanning electron microscope (SEM) image where 5.5 dyads TFE layers are deposited. The Al<sub>2</sub>O<sub>3</sub> and polymer layer thicknesses are measured to be about 44 and 590 nm, respectively.

To evaluate the barrier property of the TFE films, we have conducted a Ca test and estimated the WVTR. The Ca test has been done in the same manner presented in [6]. It is based on the corrosion of thin calcium films. We have carried out the Ca test at temperature of 20 °C and a common relative humidity of 50%. As presented in Table 2, we have achieved the WVTR as low as  $2.7 \times 10^{-6}$  g/m<sup>2</sup> day, which is acceptable for lighting applications.

We have then investigated the heat transfer property of the TFE film. To this end, we have fabricated three bilayers

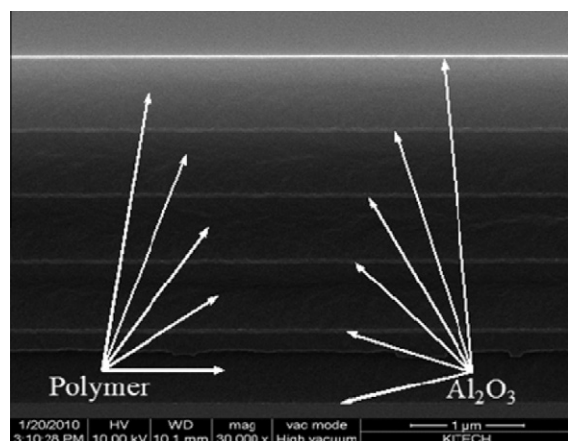
**Table 2**  
Measured WVTR of the 5.5 dyads TFE film and sample images for different time slot.

Results Time (hr)	WVTR (g/m <sup>2</sup> -day)	Sample
0		
100	2.17E-05	
200	1.10E-05	
300	9.44E-06	
400	8.43E-06	
500	2.73E-06	

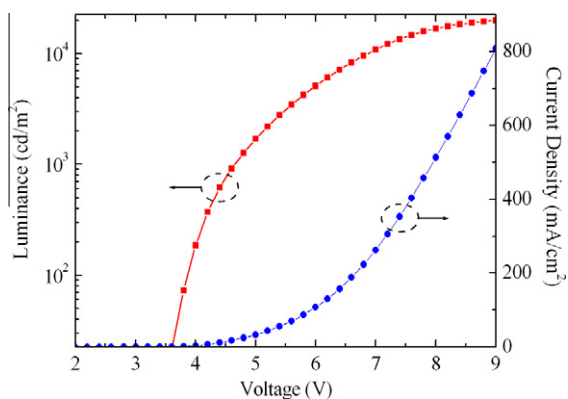
(HTL/ETL) OLEDs with different encapsulation structures (i.e., the conventional glass encapsulation, epoxy-filled glass encapsulation, and thin-film encapsulation) and made a comparative analysis of them in terms of the thermal performance. The emission area of the devices is 4.0 mm<sup>2</sup>. Fig. 3 shows the measured J–V curve of the bi-layer OLED, exhibiting the driving voltage of 4.7 V at 1000 cd/m<sup>2</sup> (21 mA/cm<sup>2</sup>) and the luminance of 14,120 cd/m<sup>2</sup> at 7.5 V (378 mA/cm<sup>2</sup>). For a comparison, we have measured the surface temperature of OLEDs without and with the flexible heat sink at a fixed voltage of 7.5 V using a thermal imager.

From Fig. 4, it is visible to the naked eye that there is no big difference in the surface temperature distribution between the glass encapsulated OLEDs with and without the heat sink. To quantify it, we have measured the transient variation of the maximum surface temperature. It is observed that the maximum surface temperature has been reduced by only 6 °C (from 55.5 °C to 49.6 °C) with the aid of the heat sink. Such a small reduction is due to the fact that there exists air (nitrogen gas) between the OLED device and the heat sink. Nitrogen gas has the thermal conductivity of 0.024 W/m K [12], which is much lower than that of glass. It hence results in poor heat transfer performance of the conventional glass encapsulation.

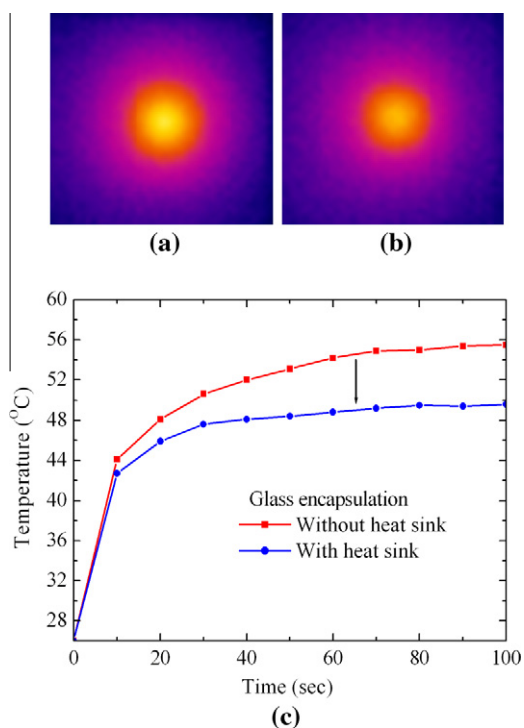
To eliminate nitrogen gas from the device, we have filled a thermally conductive epoxy resin (XNR 5570-B1, Nagase ChemteX Corp.) in the glass cover and then UV-cured it. Except for the epoxy-sealed area, the 0.7-mm-



**Fig. 2.** SEM image of 5.5 dyads TFE layers fabricated with Vitex TFE equipment.

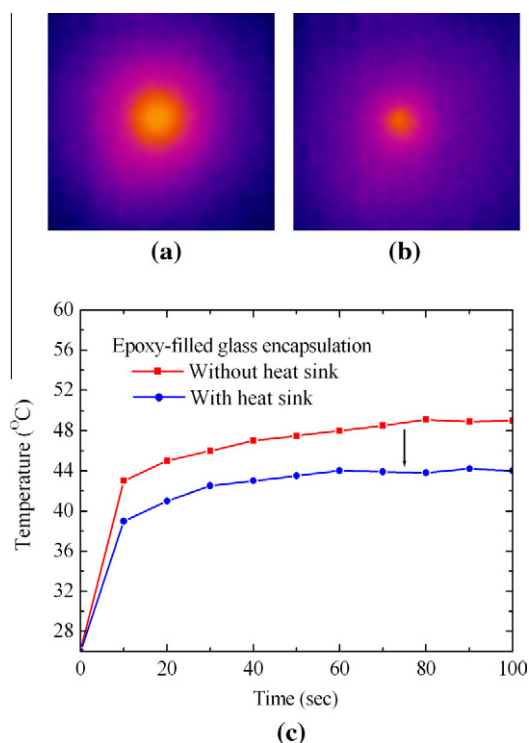


**Fig. 3.** Luminance and current density of the bilayer OLED as a function of bias voltage.



**Fig. 4.** Surface temperature distribution over the glass encapsulated OLED (a) without and (b) with heat sink, and (c) transient variation of the maximum surface temperature measured at 7.5 V.

thick glass cover is hollowed out such that its thickness becomes 0.35 mm and thus the epoxy resin can be filled therein. Just in case that epoxy causes any damage on the organic and cathode layers, we have inserted a buffer layer that consists of a 40-nm-thick NPB and 50-nm-thick LiF. For OLEDs with the epoxy-filled glass encapsulation, the maximum surface temperature is observed to be only 49 °C (Fig. 5) when the heat sink is not even involved, which is almost the same as that of the glass encapsulated OLED with the heat sink. It seems that heat transfers through the thermally conductive epoxy resin to the glass

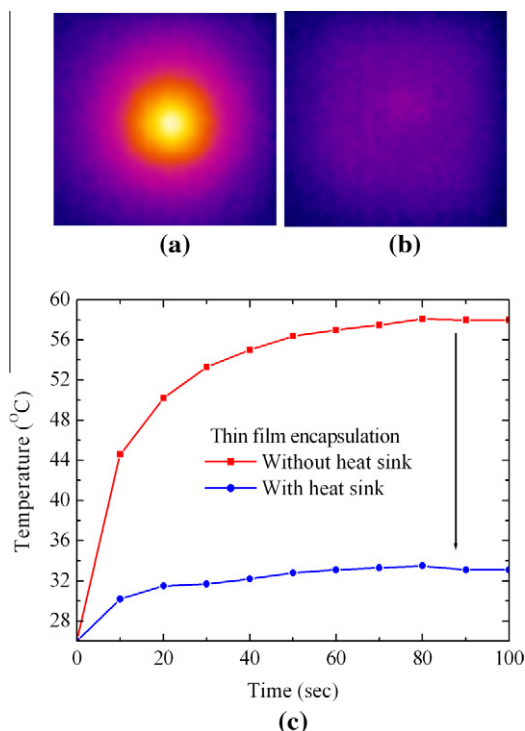


**Fig. 5.** Surface temperature distribution over the epoxy-filled glass encapsulated OLED (a) without and (b) with heat sink, and (c) transient variation of the maximum surface temperature measured at 7.5 V.

cover and then air. In fact, it is attributed that the thermal conductivity of epoxy is about 0.35 W/m K [12], which is much higher than that (0.024 W/m K) of nitrogen gas. Therefore, heat can be transferred to the surroundings even without the heat sink. However, the effect of the heat sink attached is likely to be little as the temperature reduction by the heat sink is only 5 °C (from 49 °C to 44 °C). It may be because the heat transfer pathway is very long and thus there appears a significant temperature gradient inside the thick (0.35 mm) epoxy layer, resulting from the fact that the thermal conductivity of epoxy is still low. There's plenty of room for improving its thermal performance. For instance, one may blend higher thermal conductivity materials (e.g., carbon nanotubes, Ag paste, etc.) with the epoxy. Meanwhile, the outgassing problem of this encapsulation scheme may be resolved by replacing the epoxy resin with a getter dryer such as a calcium oxide (CaO) powder.

We have then evaluated the thermal property of the thin-film encapsulated OLED. From Fig. 6, one can clearly see that the surface temperature is reduced to a great extent by the heat sink. It is observed to fall from 58 °C to 33 °C. Such a large reduction in temperature (25 °C) results from a short heat transfer pathway of the TFE structure. The total thickness of the TFE layer is only 3.2 μm. As such, heat generated in the emitting layer can be well transferred to the heat sink and dissipated by it. From this, one may jump into conclusion that the TFE structure combined with a heat sink shows the best heat transfer prop-

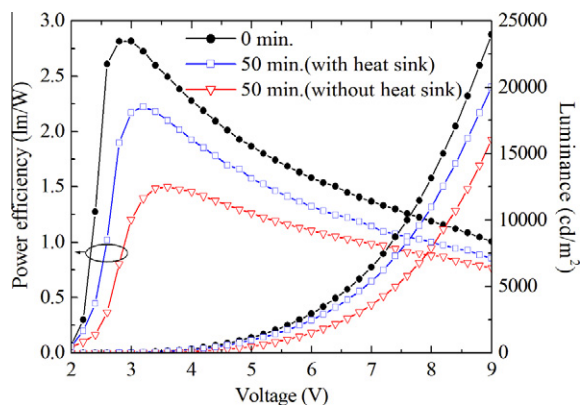




**Fig. 6.** Surface temperature distribution over the thin-film encapsulated (3.5 dyads) OLED (a) without and (b) with heat sink, and (c) transient variation of the maximum surface temperature measured at 7.5 V.

erty. Therefore, it is highly preferred for OLEDs provided that its oxygen barrier requirement is well met.

We have further investigated the positive effect of heat dissipation by the heat sink on the device performance of the thin-film encapsulated OLEDs. Shown in Fig. 7 are the power efficiency and luminance of thin-film encapsulated (3.5 dyads) OLEDs with and without heat sink as a function of bias voltage measured after 50 min of aging at 7.5 V ( $\sim 10,000$  nit). It is found that both devices exhibit a reduction of luminance and power efficiency because they were



**Fig. 7.** Power efficiency and luminance of thin-film encapsulated (3.5 dyads) OLEDs with and without heat sink as a function of bias voltage measured after 50 min of aging at 7.5 V ( $\sim 10,000$  nit).

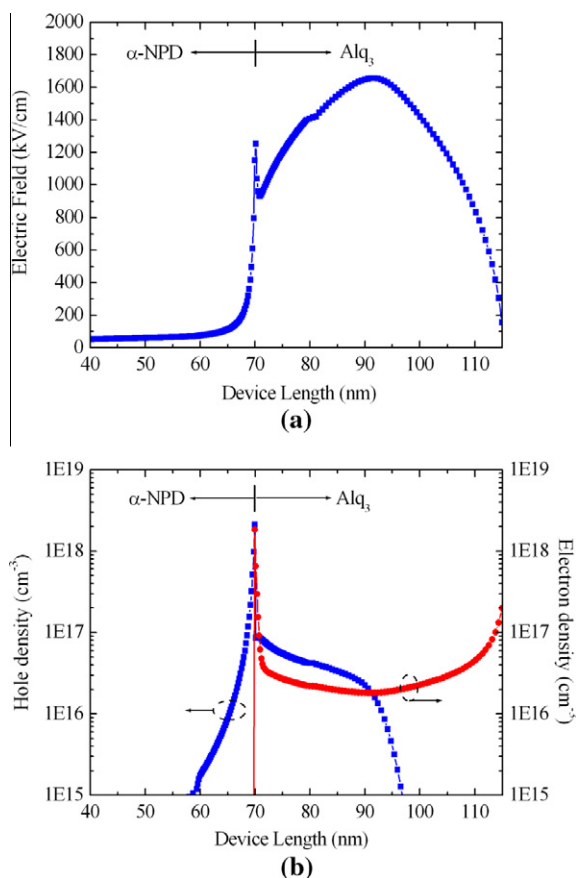
operated at high luminous intensity. However, less performance degradation appears in the device with heat sink due most likely to effective heat dissipation (Fig. 6). As such, it is desirable to employ a heat sink when OLEDs are operated at high luminance in order to reduce the unwanted Joule heating effect.

It is known that the heat transfer performance could be degraded if a multi-heterojunction is involved (namely, various different types of materials are interfaced) in the TFE structure and/or a polymer material used in the TFE film has low thermal conductivity. To verify it, we have simulated the heat transfer property of the TFE structure (Fig. 1) using the model introduced in Section 2. Summarized in Table 3 are the parameter values of thermal conductivity of those layer materials, which are required for simulations. The thermal conductivity of the polymer in the TFE film is assumed to be the same as that of the organic materials. For simplicity, we also make an assumption that the thermal conductivity of  $\alpha$ -NPD is the same as that of Alq<sub>3</sub>. By way of simulations, one can visualize where severe heat generation occurs inside the device. From Eqs. (3) and (6), the induced high carrier concentration along with the electric field is known to generate severe heat in the organic films. As presented in Fig. 8 showing the simulation results of the electric field and carrier density distributions inside the device, steep carrier accumulation takes place at the organic/organic interface and high electric field is induced near the interface inside the ETL layer, where severe heat is generated.

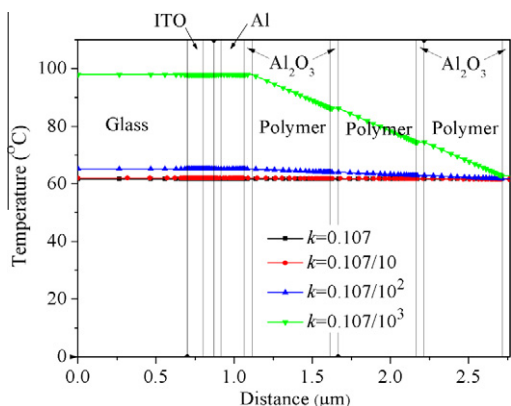
With attempt to investigate the effect of the thermal conductivity of the polymer layer on the heat transfer property, we have intentionally reduced its thermal conductivity from 0.107 W/m K to  $0.107 \times 10^{-3}$  W/m K and performed simulations of the spatial heat distribution without and with the heat sink. As shown in Figs. 9 and 10, when the thermal conductivity of the polymer is equal to 0.107 W/m K (i.e., it is close to the real value of the polymer conductivity), the simulation results of the surface temperature (61.7 °C without heat sink and 27.03 °C with heat sink) are very close to the measured ones (58 °C without heat sink and 33 °C with heat sink), validating our numerical calculations. It is observed that the temperature rises up with reduced thermal conductivity of the polymer. Consequently, there appears a significant temperature gradient inside the TFE layers. However, there will not arise a steep temperature gradient inside the TFE layers once the thermal conductivity of a polymer material is higher than  $0.107 \times 10^{-2}$  W/m K, which offers a wide choice of a polymer material. Since not many materials have such a low

**Table 3**  
Thermal conductivity values.

Layer	$k$ (W/m K)
Glass	1.05 [12]
ITO	12 [21]
$\alpha$ -NPD	0.107
Alq <sub>3</sub>	0.107 [22]
Al	250 [12]
Al <sub>2</sub> O <sub>3</sub>	30 [12]
Polymer	0.107
Copper	401 [12]



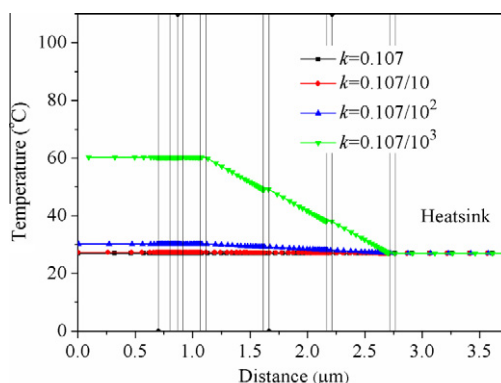
**Fig. 8.** Simulation results of (a) electric field and (b) carrier density distributions inside the bilayer OLED structure at 7.5 V.



**Fig. 9.** Simulation results of temperature distribution over the thin-film encapsulated OLED without heat sink at 7.5 V.

thermal conductivity in reality, it can be concluded that the effect of a low thermal conductivity polymer material on the thermal performance of the TFE structure is negligible.

To find whether or not the multi-heterojunction configuration affects the thermal performance of the TFE film, we have further measured the maximum surface temperature



**Fig. 10.** Simulation results of temperature distribution over the thin-film encapsulated OLED with heat sink at 7.5 V.

**Table 4**

Measured and simulated maximum surface temperatures for different TFE structures without heat sink at 7.5 V.

	1.5 dyads	3.5 dyads	5.5 dyads
Measurement	59.1	58	58.7
Simulation	61.5	61.7	61.9

by varying the TFE structure. Namely, we have reduced the number of TFE dyads to 1.5 or increased it up to 5.5. As presented in Table 4, there is no big difference in the temperature. It means that though the TFE structure is based on the multi-heterojunction configuration, yet no significant degradation in the heat transfer performance is brought in since the overall thickness of the TFE film is very small, which is also supported by the simulation results in Table 4.

#### 4. Conclusion

We have made a comparative analysis of the thermal performance of three different encapsulation schemes; namely, the conventional glass encapsulation, epoxy-filled glass encapsulation, and thin-film encapsulation. It has been found that, in the presence of a slim and flexible heat sink, the thin-film encapsulation shows the best thermal performance, followed by the epoxy-filled glass encapsulation and then the conventional glass encapsulation. By way of experiments and simulations, we have verified that the multi-heterojunction configuration and/or the low thermal conductivity of a polymer material in the TFE film have no impact on the thermal performance due to its extremely short heat transfer pathway.

#### Acknowledgement

This work was supported by the IT R&D program of MKE/IITA. (2009-F-016-01, Development of Eco-Emotional OLED Flat-Panel Lighting).

#### References

- [1] S. Reineke, F. Lindner, G. Schwartz, N. Seidler, K. Walzer, B. Lüssem, K. Leo, *Nature* 4759 (2009) 234.

- [2] Joerg Amelung, <http://spie.org/x23960.xml>
- [3] P.E. Burrows, V. Bulovic, S.R. Forrest, L.S. Sapochack, D.M. McCarty, M.E. Thompson, Appl. Phys. Lett. 65 (1994) 2922.
- [4] J.D. Affinito, M.E. Gross, C.A. Coronado, G.L. Graff, E.N. Greenwell, P.M. Martin, Thin Solid Films 290–291 (1996) 63.
- [5] A.P. Ghosh, L.J. Gerenser, C.M. Jarman, J.E. Fornalik, Appl. Phys. Lett. 86 (2005) 223503–1.
- [6] G. Nisato, M. Kuilder, P. Bouten, L. Moro, O. Philips, N. Rutherford, SID 00 Digest XXXIV, 2003, p. 88.
- [7] J. Meyer, D. Schneidenbach, T. Winkler, S. Hamwi, T. Weimann, P. Hinze, S. Ammermann, H.-H. Johannes, T. Riedl, W. Kowalsky, Appl. Phys. Lett. 94 (2009) 233305–1.
- [8] A.B. Chwang, M.A. Rothman, S.Y. Mao, R.H. Hewitt, M.S. Weaver, J.A. Silvernail, K. Rajan, M. Hack, J.J. Brown, X. Chu, L. Moro, T. Krajewski, N. Rutherford, Appl. Phys. Lett. 83 (2003) 413.
- [9] F.L. Wong, M.K. Fung, S.L. Tao, S.L. Lai, W.M. Tsang, K.H. Kong, W.M. choy, C.S. Lee, S.T. Lee, J. Appl. Phys. 104 (2008) 014509–1.
- [10] G.L. Graff, R.E. Williford, P.E. Burrows, J. Appl. Phys. 96 (2004) 1840.
- [11] C. Charton, N. Schiller, M. Fahland, A. Hollander, A. Wedel, K. Noller, Thin Solid Films 502 (2006) 99.
- [12] [http://www.engineeringtoolbox.com/thermal-conductivity-d\\_429.html](http://www.engineeringtoolbox.com/thermal-conductivity-d_429.html)
- [13] B. Ruhstaller, S.A. Carter, S. Barth, H. Riel, W. Riess, J.C. Scott, J. Appl. Phys. 89 (2001) 4575.
- [14] B. Ruhstaller, T. Beierlein, H. Riel, S. Karg, J.C. Scott, W. Riess, IEEE J. Sel. Top. Quantum Electron. 9 (2003) 723.
- [15] J.W. Park, Y. Kawakami, IEEE/OSA J. Display Tech. 2 (2006) 333.
- [16] J.W. Park, Y. Kawakami, S.H. Park, IEEE/OSA J. Lightwave Technol. 25 (2007) 2828.
- [17] P.W.M. Blom, M.J.M. de Jong, S. Breedijk, Appl. Phys. Lett. 71 (1997) 930.
- [18] J.M. Lupton, I.D.W. Samuel, J. Phys. D: Appl. Phys. 32 (1999) 2973.
- [19] G.G. Malliaras, J.C. Scott, J. Appl. Phys. 83 (1998) 5399.
- [20] <http://polynetwork.asia/eindex.html>
- [21] [http://thinfilmproducts.umicore.com/pdf/datenblatt\\_ito.pdf](http://thinfilmproducts.umicore.com/pdf/datenblatt_ito.pdf)
- [22] M.W. Shin, H.C. Lee, K.S. Kim, S.H. Lee, J.C. Kim, Thin Solid Films 363 (2000) 244.